Journal of Advanced Research (2016) 7, 1035–1044

Cairo University

Journal of Advanced Research

ORIGINAL ARTICLE

Response surface and neural network based predictive models of cutting temperature in hard turning

Mozammel Mia [a,*], Nikhil R Dhar [b]

[a] Mechanical and Production Engineering, Ahsanullah University of Science and Technology, Dhaka 1208, Bangladesh
[b] Department of Industrial and Production Engineering, Bangladesh University of Engineering and Technology, Dhaka 1000, Bangladesh

GRAPHICAL ABSTRACT

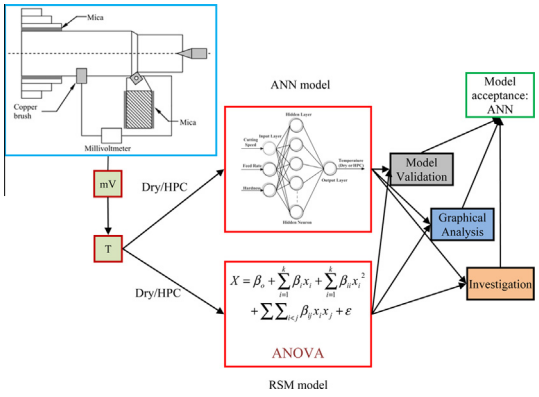

ARTICLE INFO

Article history:
Received 12 April 2016
Received in revised form 10 May 2016
Accepted 15 May 2016
Available online 24 May 2016

ABSTRACT

The present study aimed to develop the predictive models of average tool-workpiece interface temperature in hard turning of AISI 1060 steels by coated carbide insert. The Response Surface Methodology (RSM) and Artificial Neural Network (ANN) were employed to predict the temperature in respect of cutting speed, feed rate and material hardness. The number and orientation of the experimental trials, conducted in both dry and high pressure coolant (HPC)

* Corresponding author. Tel.: +880 1689449864.
E-mail addresses: arif_ipe@yahoo.com, mozammel.mpe@aust.edu (M. Mia).

Peer review under responsibility of Cairo University.

ELSEVIER Production and hosting by Elsevier

http://dx.doi.org/10.1016/j.jare.2016.05.004

Keywords:
Hard turning
Tool-workpiece interface temperature
Response surface methodology
Artificial neural network
High pressure coolant

environments, were planned using full factorial design. The temperature was measured by using the tool-work thermocouple. In RSM model, two quadratic equations of temperature were derived from experimental data. The analysis of variance (ANOVA) and mean absolute percentage error (MAPE) were performed to suffice the adequacy of the models. In ANN model, 80% data were used to train and 20% data were employed for testing. Like RSM, herein, the error analysis was also conducted. The accuracy of the RSM and ANN model was found to be $\geqslant$99%. The ANN models exhibit an error of ~5% MAE for testing data. The regression coefficient was found to be greater than 99.9% for both dry and HPC. Both these models are acceptable, although the ANN model demonstrated a higher accuracy. These models, if employed, are expected to provide a better control of cutting temperature in turning of hardened steel.

Introduction

The hard machining inherently possesses some of the major difficulties during the machining runs so as to hinder the process of achieving a higher quality of the product. Among several factors, cutting temperature is considered as the main culprit to ignite the difficulties. The adverse conditions, aroused from machining of hard material, can be properly addressed well before the actual machining, if and only, the outcome could be known far before the actual machining. Hence the necessity of computing the temperature of tool-workpiece interface is of great prevalence. Regarding this fact, many researchers have developed different models of cutting temperature in respect of different variables such as cutting speed, feed rate, and depth of cut.

In hard turning of steels, the material is hardened first, by proper heat treatment and, later put into the machining process to remove material and define the require shape. Herein, the metal cutting mechanics act differently than the machining of non-hardened steels. Drastic rise of temperature, in absence of cooling and lubrication, causes a detrimental effect on the tool and work material including the change in the microstructure. Karpat and Özel [1] analytically modeled the cutting temperature along with temperature distribution over the tool surface and found a good agreement between the experimental and predicted temperature. Liang et al. [2] developed an improved 3D model of chip-tool interface temperature in turning process of AISI 1045 steel by considering inverse heat conduction method. Pervaiz et al. [3] modeled cutting temperature of turning tool by considering the effect of flowing air surrounding the insert and the result helped to better understand the temperature scheme.

Sharma et al. [4] developed the optimization model of cutting temperature in turning AISI D2 steel under the application of different fluids using Taguchi method. The result revealed that the carbon nanotubes, when used with fluid, reduced cutting temperature effectively owing to the increase in heat transfer rate. Davoodi and Tazehkandi [5] investigated experimentally and optimized, using RSM, the cutting temperature in turning with an objective to eliminate cutting fluid. Yang and Natarajan [6] optimized the turning process parameters for the minimum tool wear and maximum material removal rate but without upsetting the cutting temperature limit. In other study, Umer et al. [7] optimized the cutting temperature using genetic algorithm but without compromising the power to cut and material removal rate. Moura et al. [8] investigated the capability of solid lubricant in reduction of chip-tool interface temperature during turning and concluded that the better lubrication is achieved with solid lubricant in suspension with oil.

The study on the application of cutting fluid, to reduce the cutting temperature, and consequently, lessen the adverse effects on the performances such as reduced tool wear, cutting force, and surface roughness, has been carried out by many researchers. Different fluid application methods such as minimum quantity lubricant [9,10], high pressure coolant [11,12], and cryogenic [13,14] establish themselves as viable alternative to dry cutting. Very few models [15,16] of chip-tool interface temperature have been developed by considering the machining environments/parameters. Hence, to better control the machining process, the prediction of cutting temperature is inevitable. To meet this objective, in this work, the response surface method and artificial neural network have been employed to model the cutting temperature in respect of cutting speed, feed rate and material hardness. It is also mentionable, using these methods, very few has incorporated material hardness as the input variable.

Methodology

Machine, method and equipment

In this work, three shafts of AISI 1060 steel (L = 200 mm, O. D. = 120 mm, I.D. = 45 mm) have been heat treated to achieve three hardness (H) values i.e. 40 HRC, 48 HRC and 56 HRC. The thermal treatment is performed in an induction furnace with appropriate heating element: firstly – by rising the temperature to 900 °C and holding at that temperature for 90 min, then suddenly reducing the temperature by oil quenching to attain a very high hardness, lastly – by raising the temperature to 375 °C, 235 °C and 150 °C for respective workpieces to remove excess hardness and brittleness. The results of hardness test are plotted in Fig. 1.

A powered center lathe (7.5 kW) was used to carry out the experimental runs on dry and high pressure coolant (HPC) applied turning. A sophisticated high pressure coolant supply system [12] has been employed to impinge the cutting oil to the tool-workpiece contact point. The cutting oil was supplied at 80 bar pressure, at a flow rate of 6 l/min, through external nozzle of 0.5 mm diameter. For better penetration and lubrication, the oil jet was aimed along the auxiliary cutting edge so that oil can reach under the flowing chips [11]. The coated (with TiCN, WC, Co) carbide insert (ISO specification-SNMM 120408) placed on PSBNR 2525 M12 holder has been used. The cutting speed (Vc) and feed rate (So) were chosen, keeping in mind the recent industrial practice, as 58, 81, 115 m/min and 0.10, 0.12, 0.14 mm/rev respectively. The depth of cut was maintained constant at 1.0 mm. These variables are oriented into 54 experimental runs (27 for dry cutting and 27

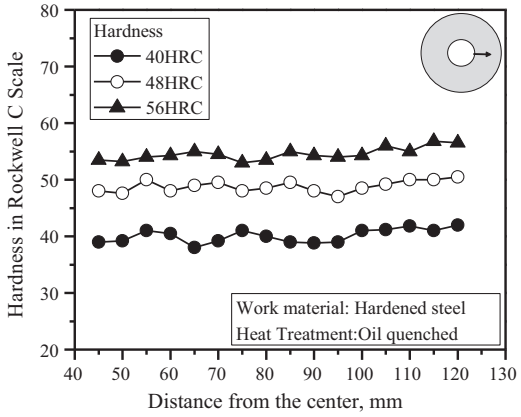

Fig. 1 Results of hardness test along radius.

for HPC cutting) generated by the full factorial design plan. Table 1 shows the experimental plan along with the measured cutting temperature. The photographic view of the experimental setup is shown in Fig. 2.

The average tool-workpiece interface temperature was measured by using a sophisticated tool-work thermocouple [17]. The calibration setup and equipments of the thermocouple are shown in Fig. 3(a) [18]. The chip of AISI 1060 steel (work material) and tungsten carbide (tool material) was joined to create the junctions of the thermocouple. Since there is possibility of parasitic electromotive force (EMF) initiation, an extension of the tool insert was produced by the carbide rod. A graphite block has been used as the heat sink. This block was surrounded by a heated porcelain tube. The temperature of a junction was measured by using a k-type thermocouple which was considered as the reference temperature. At the same time, the EMF (of the developed thermocouple) was measured by using a digital multi-meter. Then, a relation of the measured temperature and the generated EMF was plotted, as shown in Fig. 3(b), wherein the correlation coefficient was found to be 0.999. Therefore, this tool-work thermocouple is proved to be usable. Finally, the temperature of the cutting edge of the tool was measured by following the previously mentioned facts. The machining runs were conducted for a certain amount of time so that the generated EMF reaches at a stable value and only then that EMF was recorded. The schematic diagram of the temperature measurement circuit is displayed in Fig. 4.

Response surface model

The response surface methodology is a statistical tool that formulates a defined relation between two sets of data, wherein one set is dependent variable and the other sets are independent variables, along with mathematical correlation [19]. This model can determine the interaction effects of variables on the output quality. Among the versatilities of RSM, the prediction and optimization capabilities are highly appreciated. Furthermore, RSM is capable of generating both linear and quadratic models as shown in Eq. (1) and (2):

$$X = \beta_o + \beta_1 x_1 + \beta_2 x_2 + \ldots + \beta_n x_n + \varepsilon \quad (1)$$

Table 1 Experimental design plan and cutting temperature.

SL no	Cutting speed, V_c m/min	Feed rate, S_o mm/rev	Hardness, H HRC	Temperature, °C		Status
				Dry	HPC	
1	58	0.1	40	700	595	Training
2	58	0.1	48	735	635	Testing
3	58	0.1	56	920	792	Training
4	58	0.12	40	726	632	Training
5	58	0.12	48	761	672	Training
6	58	0.12	56	958	835	Training
7	58	0.14	40	764	670	Testing
8	58	0.14	48	799	710	Training
9	58	0.14	56	996	920	Training
10	81	0.1	40	750	645	Training
11	81	0.1	48	785	685	Training
12	81	0.1	56	976	875	Training
13	81	0.12	40	750	660	Training
14	81	0.12	48	785	700	Training
15	81	0.12	56	998	892	Testing
16	81	0.14	40	805	708	Training
17	81	0.14	48	840	748	Training
18	81	0.14	56	1035	942	Training
19	115	0.1	40	809	725	Training
20	115	0.1	48	844	765	Training
21	115	0.1	56	1064	932	Testing
22	115	0.12	40	833	746	Training
23	115	0.12	48	868	786	Training
24	115	0.12	56	1098	972	Training
25	115	0.14	40	854	770	Testing
26	115	0.14	48	889	810	Training
27	115	0.14	56	1150	1045	Training

Fig. 2 Photographic view of the experimental setup.

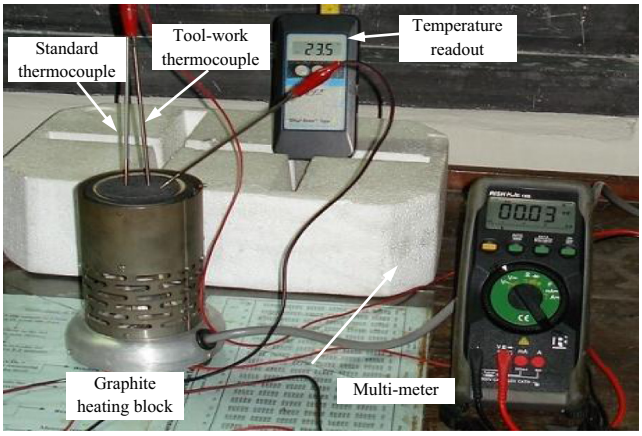

(a) Calibration setup

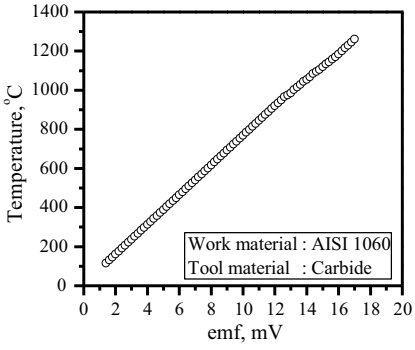

(b) Relation of temperature with generated EMF

Fig. 3 Calibration of tool-work thermocouple.

$$X = \beta_o + \sum_{i=1}^{k} \beta_i x_i + \sum_{i=1}^{k} \beta_{ii} x_i^2 + \sum \sum_{i<j} \beta_{ij} x_i x_j + \varepsilon \quad (2)$$

where X is the quality response – cutting temperature for dry or HPC; β_o is the fixed term; $\beta_1, \beta_2, \ldots, \beta_n$ in Eq. (1) are the coefficients of the linear terms; β_i, β_{ii}, β_{ij} in Eq. (2) are the coefficient of linear, quadratic and cross-product terms, respectively; x_i is the input variables (i.e. cutting speed, feed rate and material hardness).

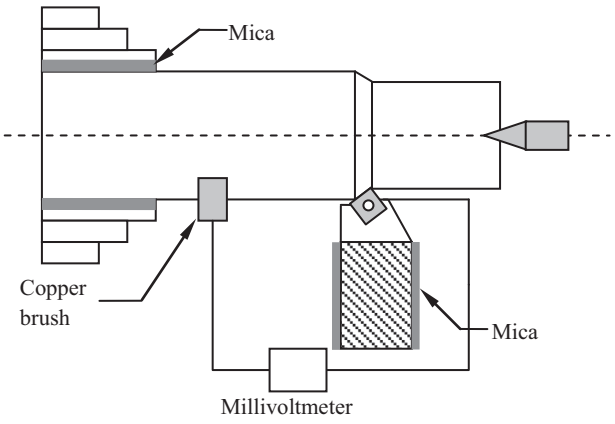

Fig. 4 Tool-work thermocouple circuit for measuring temperature.

Artificial neural network model

Artificial neural network is formed as a non-linear mapping system that works like human brain wherein a total of three layers are interconnected and each layer has one or more neurons. First layer, named input layer, receives numerical values as input to the model. Herein, one neuron is defined by one variable. Second layer, i.e. hidden layer, receives the information from the input layer and processes further. Output layer, connected with hidden layer by synaptic weights, provides the output(s). The type of configuration, training algorithm, different functions, and weights and biases influence the accuracy of the ANN model.

In this work, a feed forward multi-layer neural network, for both dry and HPC cutting, having '3-n-1' architecture has been adopted. A major problem in designing a neural network is establishing the optimal number of layers and number of neurons to achieve the most accurate results. The number of hidden layers can be increased up to three layers and this might help to achieve high accuracy but complexity of the neural network and training time will eventually increase along with waste of computer memory; again, unnecessary increment in the neurons or layer will lead to over-fitting problem [20]. As by using only one hidden layer in this study, high prediction accuracy has been observed, so no further hidden layer was added to check the performance. The ANN architecture is shown in Fig. 5. The '3-n-1' symbolizes that the input layer is comprised of three neurons; hidden layer has n (unknown) neurons; and output layer has only neuron. The three input neurons are for cutting speed, feed rate and material hardness, whereas the single output neuron represents the tool-workpiece interface temperature. Among 27 experimental data sets, 22 sets have been used for training and 5 sets for testing the model.

MATLAB R2015a 'nnstart' wizard has been used to develop, train and test the cutting temperature prediction model. The network has been trained by using Bayesian regularization (trainbr). Bayesian regularization (BR) was developed by MacKay [21] to deal with the imprecise noisy data and it possesses the ability to prevail over the under/over fitting issue. In BR, the weights and biases are random variables [21] and the optimum weights are used [22]. Moreover,

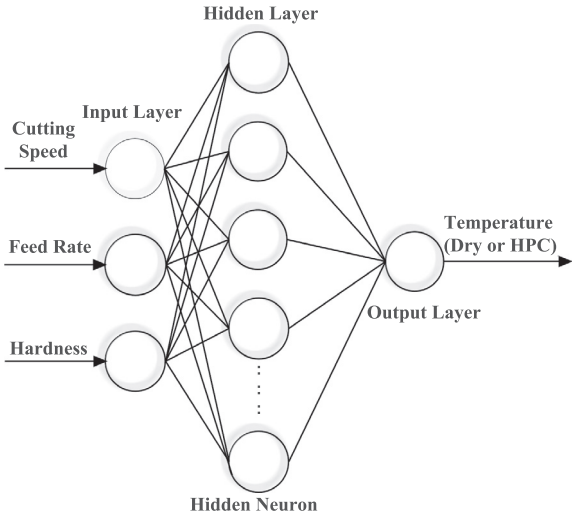

Fig. 5 3-n-1 ANN architecture.

artificial neural networks trained by adopting BR ignore the lengthy cross-validation process; it is also blessed with the ability to handle imprecise noisy data [22–24]. It takes more time to train but in case of operating with low amount of training data it can produce more accurate results than Levenberg–Marquardt algorithm. Because of the symmetric nature, transfer function Hyperbolic tangent sigmoid (tansig) has been used in hidden layer, whereas the pure linear function (purelin) has been employed in output layer. The performance was evaluated in training by mean square error (MSE) as shown in Eq. (3) and in testing by mean absolute percentage error (MAPE) as shown in Eq. (4).

$$\mathrm{MSE} = \frac{1}{N}\sum_{n=1}^{N}(Actual - Predicted)^2 \tag{3}$$

$$\mathrm{MAPE} = \frac{1}{N}\sum_{n=1}^{N}\left(\frac{|Actual - Predicted|}{Actual}\right) \times 100 \tag{4}$$

Results and discussion

In the present work, two full quadratic equations – one for dry cutting and another for high pressure coolant assisted cutting, in the form of Eq. (2), are formulated by using response surface methodology and are shown in Eq. (5) and (6) respectively. The experimental values of cutting temperature corresponding to control variables are incorporated into the RSM model in Minitab 16.0. The values of the regression coefficients for the dry and HPC models are shown in Table 2.

$$\begin{aligned}\theta_{dry} = {} & 3578.88 - 1.34728\,V_c - 4957.36\,S_o - 123.639\,H \\ & + 0.00833819\,V_c^2 + 22361.1\,S_o^2 + 1.36632\,H^2 \\ & - 3.65322\,V_cS_o - 0.0497906\,V_cH - 29.6875\,S_oH\end{aligned} \tag{5}$$

$$\begin{aligned}\theta_{HPC} = {} & 3060.42 + 1.22494\,V_c - 6477.18\,S_o - 106.421\,H \\ & + 0.00651102\,V_c^2 + 25277.8\,S_o^2 + 1.15799\,H^2 \\ & - 9.94798\,V_cS_o + 0.0201493\,V_cH + 65.1042\,S_oH\end{aligned} \tag{6}$$

The effects of different variables on the dependent variable (cutting temperature) are evaluated by the analysis of variance (ANOVA). The ANOVA for dry and HPC regression models is listed in Table 3. The ANOVA table consists of sequential sum of square from which the percentage contribution of factors is determined, *F*-value and *P*-value. The *P*-value indicates the significance of a factor to a confidence level of 95%. The higher *F*-value indicates a relatively greater importance of that factor.

For RSM quadratic dry model, the cutting speed, feed rate and material hardness, all are statistically significant as *P*-value less than 0.05. The square terms of hardness and feed rate are also significant. In addition, the only significant interaction is the cutting speed-material hardness. The *F*-value analysis reveals the material hardness as the most important factor followed by the cutting speed and then the feed rate. The highest percentage contribution is exerted by material hardness. In HPC quadratic model, the cutting speed, feed rate and material hardness are statistically significant. Like dry model, a similar significance is observable for the quadratic terms. Unlike dry model, only the feed rate-material hardness interaction is statistically significant. The percentage contribution shows that the highest (64.23%) contribution is created by material hardness, followed by cutting speed (18.51%) and lastly by the feed rate. *F*-value also revealed similar effect.

The regression plot of actual and predicted cutting temperature for RSM model is shown in Fig. 6. The values of the regression coefficient, for dry and HPC models respectively, are 0.99988 and 0.99966 and these values reflect that the model is adequate to predict the tool-workpiece interface temperature for both the machining environments. RSM is showing a better accuracy in dry cutting than the HPC assisted cutting temperature prediction. Yet, RSM is applicable to develop model in both dry and HPC cutting.

Fig. 7 shows the perturbation plots of cutting temperature for dry and high pressure coolant cutting. For both these figures the reference point is feed rate 0.12 mm/rev, cutting speed 85.66 m/min, and material hardness of 48 HRC. Herein, the material hardness and feed rate have been appeared as the most important factors.

Fig. 8 shows the three dimensional response surface plots of cutting temperature. Fig. 8(a) shows the relation of the cutting temperature with the feed rate and cutting speed while Fig. 8 (b) illustrates the temperature with cutting speed and material hardness. In dry and HPC cutting, the low feed rate and cutting speed are found to be attached with the low cutting temperature and high cutting temperature is generated at the high feed rate and cutting speed. Similarly, low hardness value produces low cutting temperature. For all the cases, the high pressure coolant reduces the cutting temperature.

The regression plot of the actual and ANN predicted cutting temperature is shown in Fig. 9. From this plot, the value of the regression coefficient is found more than 99.9% which strongly justifies the acceptability in the prediction capability of the models. In case of dry ANN model, the regression coefficient has a higher value; hence, it is conclusive that this model is more accurate than the HPC model. However, both the models can be employed in the cutting temperature prediction.

The results of the prediction of cutting temperature by RSM and ANN are shown in Table 4. In addition, the associated absolute percentage errors (APE) are calculated. Finally, the mean absolute percentage errors (MAPE) for all the mod-

Table 2 Regression coefficients of RSM regression models.

Models	Eqn.	*R*-square (%)	*R*-square (adjusted) (%)	*R*-square (predicted) (%)
θ_{dry}	5	99.56	99.33	98.83
θ_{HPC}	6	99.43	99.13	98.32

Table 3 Analysis of variance for tool-workpiece interface temperature.

Source	DF	Dry quadratic model					HPC quadratic model				
		Seq SS	% Cont.	*F*-value	*P*-value	Remark	Seq SS	% Cont.	*F*-value	*P*-value	Remark
Model	9	398,007	99.56	427.35	0.000	Significant	362,834	99.43	329.52	0.000	Significant
V_C	1	62,894	15.73	591.89	0.000	Significant	67,541	18.51	539.51	0.000	Significant
S_o	1	16,744	4.19	159.42	0.000	Significant	25,238	6.92	201.05	0.000	Significant
H	1	269,868	67.51	2623.0	0.000	Significant	234,384	64.23	1913.98	0.000	Significant
V_C^2	1	252	0.06	2.43	0.137	Not significant	154	0.04	1.26	0.278	Not significant
S_o^2	1	480	0.12	4.64	0.046	Significant	613	0.17	5.01	0.039	Significant
H^2	1	45,879	11.48	443.36	0.000	Significant	32,955	9.03	269.36	0.000	Significant
$V_C \times S_o$	1	53	0.01	0.51	0.485	Not significant	391	0.1	3.19	0.092	Not significant
$V_C \times H$	1	1566	0.39	15.13	0.001	Significant	256	0.07	2.10	0.166	Not significant
$S_o \times H$	1	271	0.07	2.62	0.124	Not significant	1302	0.36	10.64	0.005	Significant
Error	24	1759	0.44				2080	0.57			
Total	33	399,766	100				364,913	100			

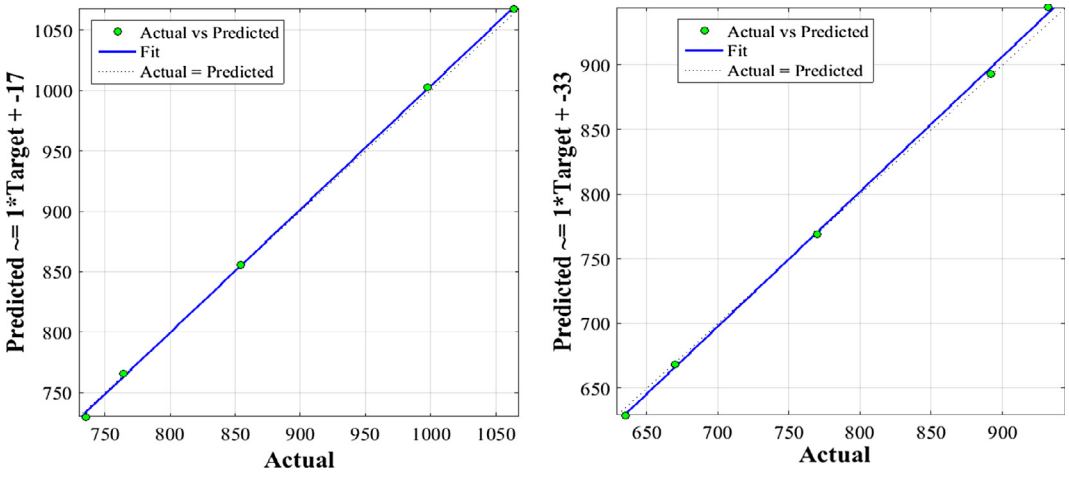

(a) Dry machining condition (R^2:0.99988) (b) HPC machining condition (R^2:0.99966)

Fig. 6 Linear regression curves for actual and RSM predicted temperature.

els are computed and shown. It can be seen that actual and predicted value of temperature are closely matched. The corresponding APE is, in most of the cases, less than one percentage. Consequently, the MAPE are less than 1 too. Hence these models are effective to predict the response within very short range of error. The dry model has a lower error rate for RSM model than the ANN model. Hence, for dry cutting the RSM model can be adopted to predict the tool-workpiece temperature. On the contrary, the HPC model reveals the superiority of the ANN model (0.69%) as the MAPE, in this case, is lower than the RSM model (0.93%). However, owing to the very low value of the MAPE, both these models are appropriate in predicting the cutting temperature.

Fig. 10 shows the comparison of the response surface model and artificial neural network model with actual cutting temperature for the testing data sets. The actual and predicted results show a good agreement between themselves. The associated mean absolute percentage error for the ANN model is also calculated. For HPC cutting, the ANN model shows higher accuracy than dry cutting.

It is noticeable from the analysis of variance shown in Table 3, carried out in RSM modeling, that the hardness is putting a dominant effect in determining the temperature at the tool-workpiece-chip interface. This is attributable to the fact that, in this work, hardened steel of very high hardness (up to 56 HRC) is machined with coated carbide insert.

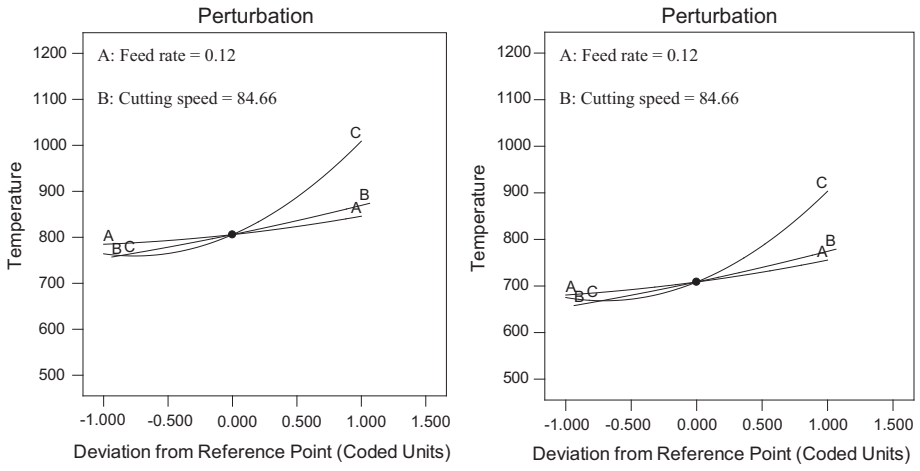

(a) Dry cutting (b) HPC cutting

Fig. 7 Perturbation plots of cutting temperature: (a) dry cutting and (b) HPC cutting.

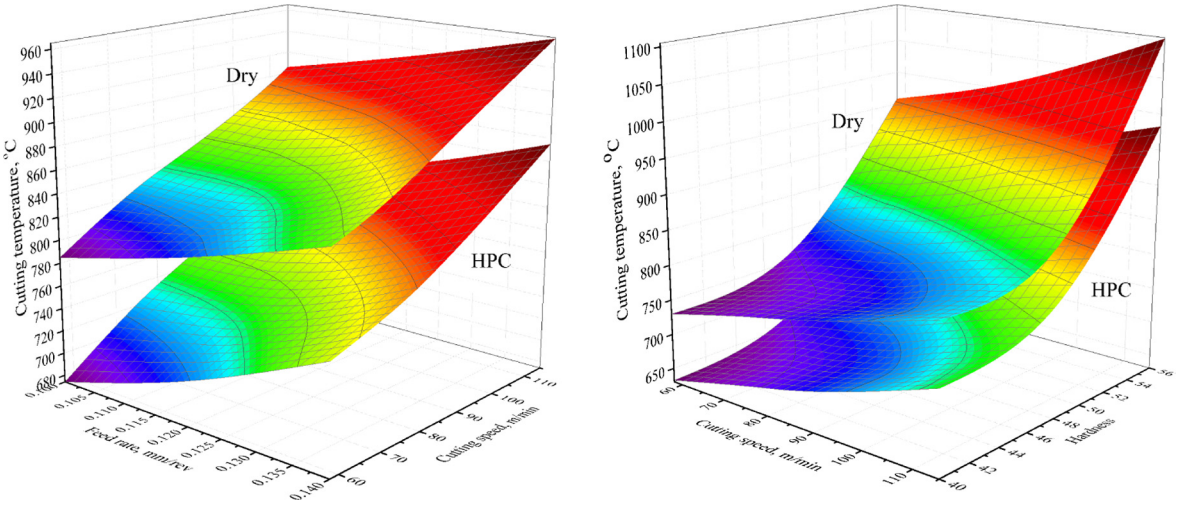

(a) Temperature vs feed-speed (b) Temperature vs speed-hardness

Fig. 8 3D response plots.

Although, coating over the tool provides some solid lubrication, yet it is not sufficient in providing perfect lubrication to reduce the effect of high friction and as there is no/minimum cooling (for dry cutting) by ambient air, a significant amount of temperature is risen in the contact point of tool-workpiece [25]. The rise of cutting temperature is due to the transfer of mechanical energy into heat energy [26] caused by the cutting tool given in the form of cutting force to deform the material plastically [8] and cut into chips. The restricting force is created by and within the material before breaking of the bonds of metals/alloy molecules against the cutting force imparted by the tool insert. The increased hardness of material gives rise to the restraining force [27] and supposedly rises the cutting temperature. Even though the application of coolant at high pressure reduces the cutting temperature and provides the lubrication [18], the change of hardness from 40 HRC to 48 HRC and then finally to 56 HRC originates different amounts of restraining force within the material and exerts severe effect on determining the cutting temperature.

Followed by material hardness, the cutting speed creates significant effect on the cutting temperature. This is because the increased cutting speed means increased amount of material removing per unit time; hence, higher friction is endured by the cutting tool which contributes to the generation of cutting temperature [28]. Furthermore, the higher cutting speed provides very short period of time to machine and within this time the cutting tool gets insufficient time to cool and consequently increases the cutting temperature [29]. When the cutting tool is hot, it becomes soft and loses its sharpness [8] and the blunt tool edge opens the higher tool contact surface (increased nose radius) and thus faces increased friction and engenders higher cutting temperature. The feed rate has little effect on the cutting temperature as the higher feed rate means a higher distance per revolution of the workpiece and this

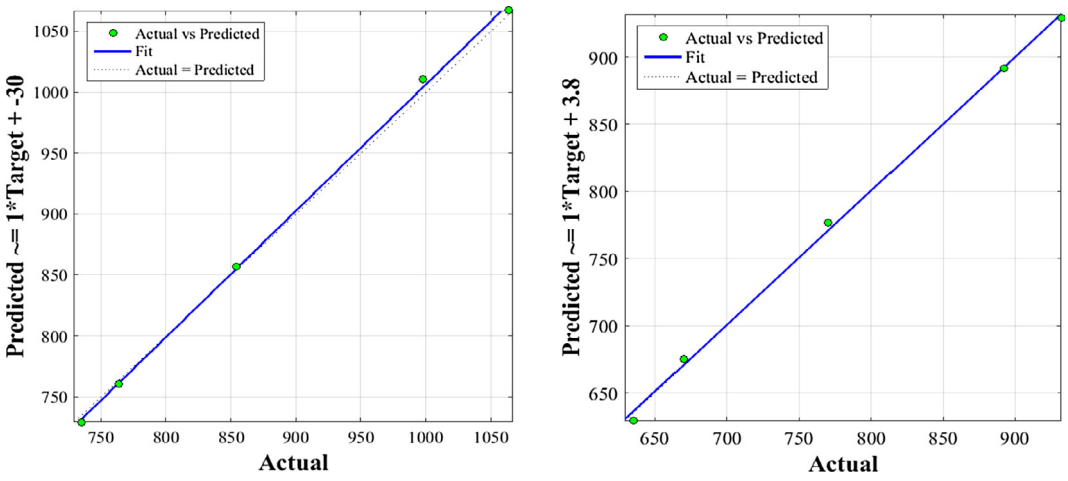

(a) Dry machining condition (R^2:0.99957) (b) HPC machining condition (R^2:0.99918)

Fig. 9 Linear regressions for actual and ANN predicted temperature.

Table 4 Performance comparison of tool-workpiece interface temperature models.

SL no	Predicted dry cutting temperature (°C)				Predicted HPC cutting temperature (°C)			
	RSM	ANN	RSM-APE (%)	ANN-APE (%)	RSM	ANN	RSM-SE (%)	ANN-SE (%)
1	710.28	706.57	1.47	0.94	603.82	597.17	1.48	0.36
2	729.90	734.86	0.69	0.02	629.10	629.02	0.93	0.94
3	924.42	926.51	0.48	0.71	802.61	790.67	1.34	0.17
4	729.03	729.71	0.42	0.51	626.04	631.15	0.94	0.13
5	753.41	759.97	1.00	0.14	661.74	662.21	1.53	1.46
6	952.67	958.81	0.56	0.08	845.66	839.74	1.28	0.57
7	765.67	754.30	0.22	1.27	668.48	675.42	0.23	0.81
8	794.80	786.99	0.53	1.50	714.60	717.39	0.65	1.04
9	998.82	992.66	0.28	0.34	908.94	915.61	1.20	0.48
10	743.35	743.03	0.89	0.93	648.46	643.74	0.54	0.20
11	772.14	773.52	1.64	1.46	677.46	683.00	1.10	0.29
12	975.82	974.99	0.02	0.10	854.67	851.92	2.32	2.64
13	760.42	769.01	1.39	2.53	666.11	665.04	0.93	0.76
14	793.96	802.70	1.14	2.25	705.52	704.60	0.79	0.66
15	1002.39	1011.05	0.44	1.31	893.15	891.65	0.13	0.04
16	795.39	795.26	1.19	1.21	703.98	701.89	0.57	0.86
17	833.68	833.05	0.75	0.83	753.80	751.33	0.78	0.45
18	1046.85	1048.2	1.14	1.28	951.85	958.28	1.05	1.73
19	808.40	803.18	0.07	0.72	727.08	727.04	0.29	0.28
20	850.73	843.43	0.80	0.07	761.55	763.33	0.45	0.22
21	1067.96	1060.91	0.37	0.29	944.25	928.94	1.31	0.33
22	822.99	827.40	1.20	0.67	737.96	744.00	1.08	0.27
23	870.07	873.66	0.24	0.65	782.85	785.99	0.40	0.00
24	1092.05	1098.66	0.54	0.06	975.96	973.85	0.41	0.19
25	855.47	850.13	0.17	0.45	769.07	776.32	0.12	0.82
26	907.30	903.03	2.06	1.58	824.37	832.16	1.77	2.74
27	1134.02	1135.28	1.39	1.28	1027.90	1043.02	1.64	0.19
		MAPE	0.78	0.86		MAPE	0.93	0.69

hardly causes any change in the cutting mechanism and thus produces low impact on the temperature.

In modeling of dry cutting temperature by RSM and ANN, the mean absolute percentage error was found to be 0.78% and 0.86% respectively. Based on the lower MAPE, the RSM model is suitable; yet, due to the fact that all 27 sets of data were used for the development of the quadratic model and that model has predicted the cutting temperature of the same 27 sets of data, the error accordingly showed lower value of MAPE. Similar insight is also application for the cutting temperature model of the high pressure coolant applied hard turning. Despite the fact that different data were used for training and testing the ANN model, the neural network based predictive model revealed fairly reasonable accuracy (MAPE < 1%).

Among different tested network structures, the 3–15–1 structure showed the highest accuracy in predicting the

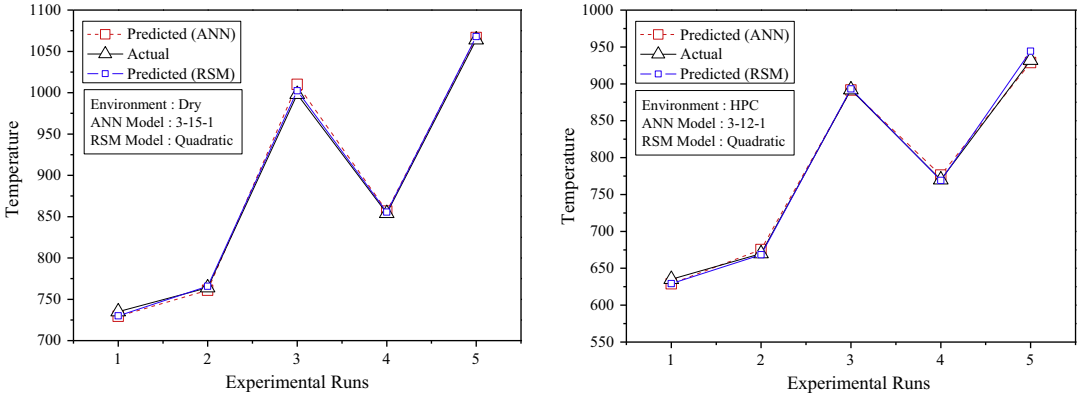

(a) Dry machining condition (b) HPC machining condition

Fig. 10 Graphical comparison of actual and predicted temperature values.

temperature during dry machining and the 3–12–1 structure revealed the minimum error in the HPC assisted hard turning. This is because of the fact that the 15 and 12 numbers of hidden neurons in the hidden layer understandably constructed the best relationship between the input and output for dry and HPC conditions respectively. The superiority of the ANN model over RSM model gets justified by the insight that the ANN forms a complex relation between the input and output corresponding to the necessity of the minimum prediction error [30], which is not attainable by the RSM as this can only form the quadratic relation between the input and the output. Hence any relation out of quadratic is non-comprehensive to RSM while ANN develops a logical relation there.

Conclusions

Based on the experiment and result analysis of the response surface and neural network based models of average cutting temperature in turning of hardened steel in respect of cutting speed, feed rate and material hardness under dry and high pressure coolant jet, the following conclusions can be drawn:

- The material hardness played an influential role on cutting temperature; yet, it was hardly considered as the quality input for the temperature prediction model. In this work, the material hardness was considered for temperature modeling along with the investigation of the effect of hardness on the cutting temperature.
- The material hardness exerted a contribution of 67% and 64% on cutting temperature for dry cutting and coolant cutting, respectively, due to an increased restraining force caused by the increased material hardness against the tool applied cutting force.
- The regression coefficients are found to be greater than 99.9% for both the RSM and ANN models and hence justify the acceptability of their prediction capability.
- The analysis of the mean absolute percentage error recommended the acceptance of the neural network based prediction model over response surface model owing to the better capability of ANN model to build an appropriate relation between the input and output.

Conflict of interest

There is no conflict of interest with the concerned persons or organizations.

Compliance with Ethics Requirements

This article does not contain any studies with human or animal subjects.

Acknowledgments

The authors are grateful to Directorate of Advisory Extension and Research Services (DAERS), BUET, Bangladesh for providing research fund, Sanction No. DAERS/CASR/R-01/2013/DR-2103 (92) dated 23/08/2014 and the Department of Industrial and Production Engineering, BUET, Dhaka, Bangladesh, for allowing laboratory facility to carry out the research work.

References

[1] Karpat Y, Özel T. Predictive analytical and thermal modeling of orthogonal cutting process—Part I: Predictions of tool forces, stresses, and temperature distributions. J Manuf Sci E 2006;128(2):435–44.
[2] Liang L, Xu H, Ke Z. An improved three-dimensional inverse heat conduction procedure to determine the tool-chip interface temperature in dry turning. Int J Therm Sci 2013;64:152–61.
[3] Pervaiz S, Deiab I, Wahba E, Rashid A, Nicolescu CM. A novel numerical modeling approach to determine the temperature distribution in the cutting tool using conjugate heat transfer (CHT) analysis. Int J Adv Manuf Technol 2015;80(5–8):1039–47.
[4] Sharma P, Sidhu BS, Sharma J. Investigation of effects of nanofluids on turning of AISI D2 steel using minimum quantity lubrication. J Clean Prod 2015;108:72–9.
[5] Davoodi B, Tazehkandi AH. Experimental investigation and optimization of cutting parameters in dry and wet machining of aluminum alloy 5083 in order to remove cutting fluid. J Clean Prod 2014;68:234–42.

[6] Yang S, Natarajan U. Multi-objective optimization of cutting parameters in turning process using differential evolution and non-dominated sorting genetic algorithm-II approaches. Int J Adv Manuf Technol 2010;49(5–8):773–84.
[7] Umer U, Qudeiri JA, Hussein HAM, Khan AA, Al-Ahmari AR. Multi-objective optimization of oblique turning operations using finite element model and genetic algorithm. Int J Adv Manuf Technol 2014;71(1–4):593–603.
[8] Moura RR, da Silva MB, Machado ÁR, Sales WF. The effect of application of cutting fluid with solid lubricant in suspension during cutting of Ti–6Al–4V alloy. Wear 2015;332:762–71.
[9] Dhar N, Ahmed M, Islam S. An experimental investigation on effect of minimum quantity lubrication in machining AISI 1040 steel. Int J Mach Tool Manuf 2007;47(5):748–53.
[10] Khan M, Mithu M, Dhar N. Effects of minimum quantity lubrication on turning AISI 9310 alloy steel using vegetable oil-based cutting fluid. J Mater Process Technol 2009;209 (15):5573–83.
[11] Mia M, Dhar NR. Effect of high pressure coolant jet on cutting temperature, tool wear and surface finish in turning hardened (HRC 48) steel. J Mech Eng 2015;45(1):1–6.
[12] Kamruzzaman M, Dhar N. The influence of high pressure coolant on temperature tool wear and surface finish in turning 17CrNiMo6 and 42CrMo4 steels. J Eng Appl Sci 2009;4 (6):93–103.
[13] Paul S, Dhar N, Chattopadhyay A. Beneficial effects of cryogenic cooling over dry and wet machining on tool wear and surface finish in turning AISI 1060 steel. J Mater Process Technol 2001;116(1):44–8.
[14] Dhar N, Paul S, Chattopadhyay A. Role of cryogenic cooling on cutting temperature in turning steel. J Manuf Sci E 2002;124 (1):146–54.
[15] Sultana I, Dhar N, editors. GA based multi objective optimization of the predicted models of cutting temperature, chip reduction co-efficient and surface roughness in turning AISI 4320 steel by uncoated carbide insert under HPC condition. Proc Int Conf Mech Ind Manuf Technol, MIMT; 2010.
[16] Al Masud A, Ali SM, Dhar NR, editors. Modeling of chip tool interface temperature in machining steel – an Artificial Intelligence (AI) approach. In: Proceedings of the 2011 international conference on industrial engineering and operations management Kuala Lumpur, Malaysia; 2011.
[17] Dhar N, Kamruzzaman M. Cutting temperature, tool wear, surface roughness and dimensional deviation in turning AISI-4037 steel under cryogenic condition. Int J Mach Tool Manuf 2007;47(5):754–9.
[18] Mia M, Dhar N. Optimization of surface roughness and cutting temperature in high-pressure coolant-assisted hard turning using Taguchi method. Int J Adv Manuf Technol 2016;1–15.
[19] Draper N, Smith H, Pownell E. Applied regression analysis. New York: Wiley; 1966.
[20] Karsoliya S. Approximating number of hidden layer neurons in multiple hidden layer BPNN architecture. Int J Eng Trends Technol 2012;3(6):713–7.
[21] MacKay DJ. Bayesian interpolation. Neural Comput. 1992;4 (3):415–47.
[22] Dan Foresee F, Hagan M, editors. Gauss-Newton approximation to Bayesian learning. In: Int conf neural netw; 1997.
[23] MacKay D. A practical Bayesian framework for backpropagation networks. Neural Comput. 1992;4(3):448–72.
[24] Haykin S. Neural networks and learning machines, vol. 3. Upper Saddle River: Pearson Education; 2009.
[25] Sharma V, Dogra M, Suri N. Cooling techniques for improved productivity in turning. Int J Mach Tool Manuf 2009;49 (6):435–53.
[26] da Silva M, Wallbank J. Cutting temperature: prediction and measurement methods—a review. J Mater Process Technol 1999;88(1):195–202.
[27] Kumar A, Rahman M, Ng S. Effect of high-pressure coolant on machining performance. Int J Adv Manuf Technol 2002;20 (2):83–91.
[28] Koné F, Czarnota C, Haddag B, Nouari M. Modeling of velocity-dependent chip flow angle and experimental analysis when machining 304L austenitic stainless steel with groove coated-carbide tools. J Mater Process Technol 2013;213 (7):1166–78.
[29] Molinari A, Nouari M. Modeling of tool wear by diffusion in metal cutting. Wear 2002;252(1):135–49.
[30] Gupta AK, Guntuku SC, Desu RK, Balu A. Optimisation of turning parameters by integrating genetic algorithm with support vector regression and artificial neural networks. Int J Adv Manuf Technol 2015;77(1–4):331–9.